Journal of Medicinal Chemistry

Article

pubs.acs.org/jmc

New Structure–Activity Relationships of A- and D-Ring Modified Steroidal Aromatase Inhibitors: Design, Synthesis, and Biochemical Evaluation

Carla Varela,[†] Elisiário J. Tavares da Silva,*[,†] Cristina Amaral,[‡,§] Georgina Correia da Silva,[‡,§] Teresa Baptista,[∥] Stefano Alcaro,[⊥] Giosuè Costa,[⊥] Rui A. Carvalho,[#] Natércia A. A. Teixeira,[‡,§] and Fernanda M. F. Roleira*[,†]

[†]CEF, Center for Pharmaceutical Studies, Pharmaceutical Chemistry Group, Faculty of Pharmacy, University of Coimbra, 3000-548 Coimbra, Portugal

[‡]Biochemistry Laboratory, Faculty of Pharmacy, University of Porto, Rua Jorge Viterbo Ferreira, 228, 4050-313 Porto, Portugal

[§]Institute for Molecular and Cellular Biology (IBMC), University of Porto, Rua do Campo Alegre, 823, 4150-180 Porto, Portugal

[∥]CEF, Center for Pharmaceutical Studies, Bromatology, Pharmacognosy and Analytical Sciences Group, Faculty of Pharmacy, University of Coimbra, 3000-548 Coimbra, Portugal

[⊥]CCLab, Dipartimento di Scienze della Salute, Università "Magna Græcia" di Catanzaro, Italy

[#]Department of Life Sciences, Faculty of Science and Technology, University of Coimbra, Portugal

Supporting Information

ABSTRACT: A- and D-ring androstenedione derivatives were synthesized and tested for their abilities to inhibit aromatase. In one series, C-3 hydroxyl derivatives were studied leading to a very active compound, when the C-3 hydroxyl group assumes 3β stereochemistry (**1**, IC_{50} = 0.18 μM). In a second series, the influence of double bonds or epoxide functions in different positions along the A-ring was studied. Among epoxides, the 3,4-epoxide **15** showed the best activity (IC_{50} = 0.145 μM) revealing the possibility of the 3,4-oxiran oxygen resembling the C-3 carbonyl group of androstenedione. Among olefins, the 4,5-olefin **12** (IC_{50} = 0.135 μM) revealed the best activity, pointing out the importance of planarity in the A,B-ring junction near C-5. C-4 acetoxy and acetylsalicyloxy derivatives were also studied showing that bulky substituents in C-4 diminish the activity. In addition, IFD simulations helped to explain the recognition of the C-3 hydroxyl derivatives (**1** and **2**) as well as **15** within the enzyme.

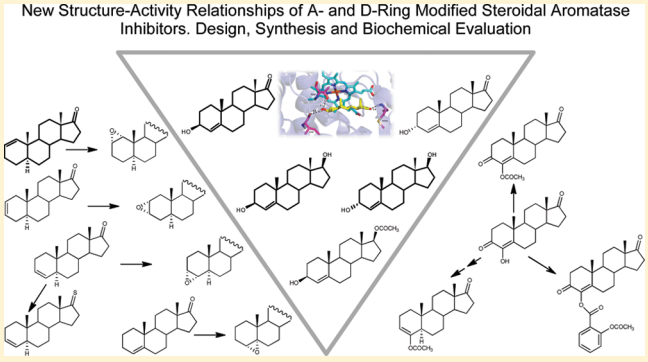

INTRODUCTION

Aromatase is a cytochrome P-450 enzyme that catalyzes the aromatization of androgens, the final step in the biosynthesis of estrogens. Aromatase inhibitors (AIs) reduce the synthesis of estrogens and offer a therapeutic alternative for the treatment of estrogen-dependent cancers such as breast cancer.[1−3] There are two classes of AIs, steroidal and nonsteroidal compounds,[4−6] which cause potent estrogen suppression.[3,7] The nonsteroidal AIs are mostly azole type compounds such as the clinically used anastrazole and letrozole, which compete with the substrate for binding to the enzyme active site. Steroidal AIs, as exemestane and formestane (**23**) (Figure 1), mimic the natural substrate androstenedione (**8**) and are converted by the enzyme in reactive intermediates, which bind irreversibly to the enzyme active site, resulting in the inactivation of aromatase. Despite the success of the third-generation nonsteroidal (anastrazole and letrozole) and steroidal (exemestane) AIs, they still have some major side effects, such as increase of bone loss, joint pain, and heart problems.[8] In addition, after some years of usage they can develop cellular resistance. For these reasons, it is important to search for other potent and specific molecules with lower side effects and which can overcome the resistance phenomena.

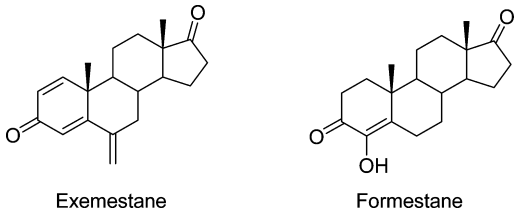

Figure 1. Steroidal aromatase inhibitors.

Received: February 21, 2012
Published: April 4, 2012

Scheme 1. Synthesis of Aromatase Inhibitors from 3 and 2[a]

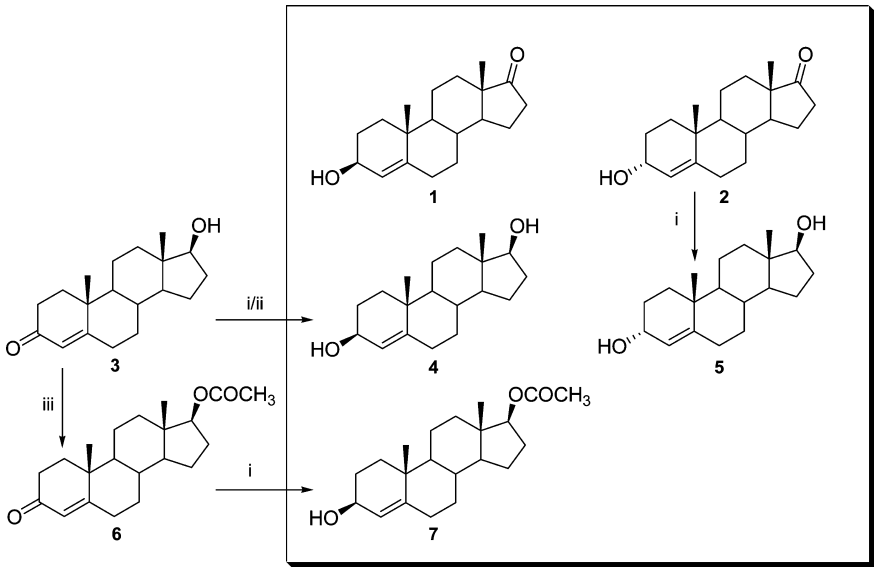

[a]Reagents and conditions: (i) $NaBH_4$, methanol, rt; (ii) $(t\text{-butoxi})_3AlLiH$, THF, reflux, 8 h 20 min; (iii) $(CH_3CO)_2O$, pyridine, rt, 21 h 25 min.

Recently, the active site of aromatase has been elucidated, and the molecular basis for enzyme–substrate interaction has been established.[9] It was found that the volume of the binding pocket taken from the enzyme–substrate complex is relatively short (no more than 400 Å^3) allowing to enter into the cleft only molecules with appropriate dimensions such as derivatives of **8** with small substituents. These findings can lead to a more rational design of new AIs and consequently to a more efficacious intervention at the level of estrogen production. Keeping this in mind, the design, synthesis, and biochemical evaluation of new substrate-based inhibitors, containing the A- and D-ring chemical key-features important for enzyme–drug interaction, would greatly contribute to establish new structure–activity relationships (SARs). These SAR are valuable tools for understanding the enzyme inhibition mechanism and to find more selective, potent, and lower side effect AIs.

Among other interactions, aromatase establishes two hydrogen bonds with the carbonyl functions at C-3 and C-17 of **8**.[9] From a previous study, it was concluded that the presence of the carbonyl group at C-3 is not mandatory to bind steroid molecules to the enzyme aromatase.[10] Other authors described AIs without the C-17 carbonyl group.[11] Recently, our group confirmed those facts and postulated that, at least, one carbonyl group (C-3 or C-17) is necessary in order to allow the binding of steroid molecules to the enzyme aromatase.[12] In the present work, one of our aims is to study steroid molecules as AIs in which the carbonyl group at C-3 (a hydrogen bond acceptor) of **8** was replaced by a hydroxyl group (a hydrogen bond donor) and also in which the two carbonyl groups (C-3 and C-17) were replaced by two hydroxyl groups. The effect of the stereochemistry of the hydroxyl group at C-3 was also explored (Scheme 1).

In our recent studies, we also noticed that some planarity in the A-ring and in the A,B-ring junction is important for the inhibitory activity of steroids against aromatase.[10,12] This planarity can be conferred by a double bond or by an epoxide function both containing similar bond geometries. Presently, we are interested in studying the influence of the position of the double bond or the epoxide function along the A-ring, in aromatase inhibitory activity. For this, we prepared two series of steroid compounds (Scheme 2) and studied their inhibitory activity against aromatase.

Compound **23** is the C-4 hydroxy analogue of **8** and was the first steroidal AI clinically used. Its C-4 acetoxy derivative **24** also revealed strong aromatase inhibitory activity.[13] Related with this, we present a preliminary SAR study based on the synthesis (Scheme 3) and aromatase inhibitory activity evaluation of C-4 acetoxy and acetylsalicyloxy derivatives of **23** and of 3,4-olefin **14** (Scheme 2), another potent AI prepared and evaluated by our team.[10]

Finally and based on the importance of the C-17 carbonyl group in steroidal AIs, the chemical modification of the C-17 carbonyl oxygen of compound **14** by its sulfur isoster **28** (Scheme 4) was performed.

Complementary docking studies by Glide/IFD simulations[14] have also been done. Actually, cytochromes P450 can adopt multiple conformations depending on the bound ligand because of the enzyme's plasticity.[15] For this reason, we generate poses of our compounds using IFD simulations, in order to take into account the binding site flexibility and to optimize the network of protein–ligand interactions as compared to rigid docking. In our analysis, we have considered the binding contributions, the induced fit effects onto the enzyme residues, and the deviation of the steroidal scaffold by the experimentally determined position of **8** with respect to the reference crystallographic model.[9]

RESULTS

Chemistry. The synthesis of the 3β-hydroxy derivative of testosterone **4** was performed through two different methods (Scheme 1). In the first approach, testosterone (**3**) reacted with sodium borohydride, in methanol, at room temperature yielding a mixture of the 3β- and 3α-isomers, which after crystallization, afforded 21% of compound **4** (Method A). In the second method, **3** was refluxed in tetrahydrofuran with lithium tri-*t*-butoxyaluminum hydride.[16] This reduction also led to a mixture of the 3β- and 3α-isomers, which after

dx.doi.org/10.1021/jm300262w | J. Med. Chem. 2012, 55, 3992–4002

Scheme 2. Synthesis of Aromatase Inhibitors from 3, 16, and 18[a]

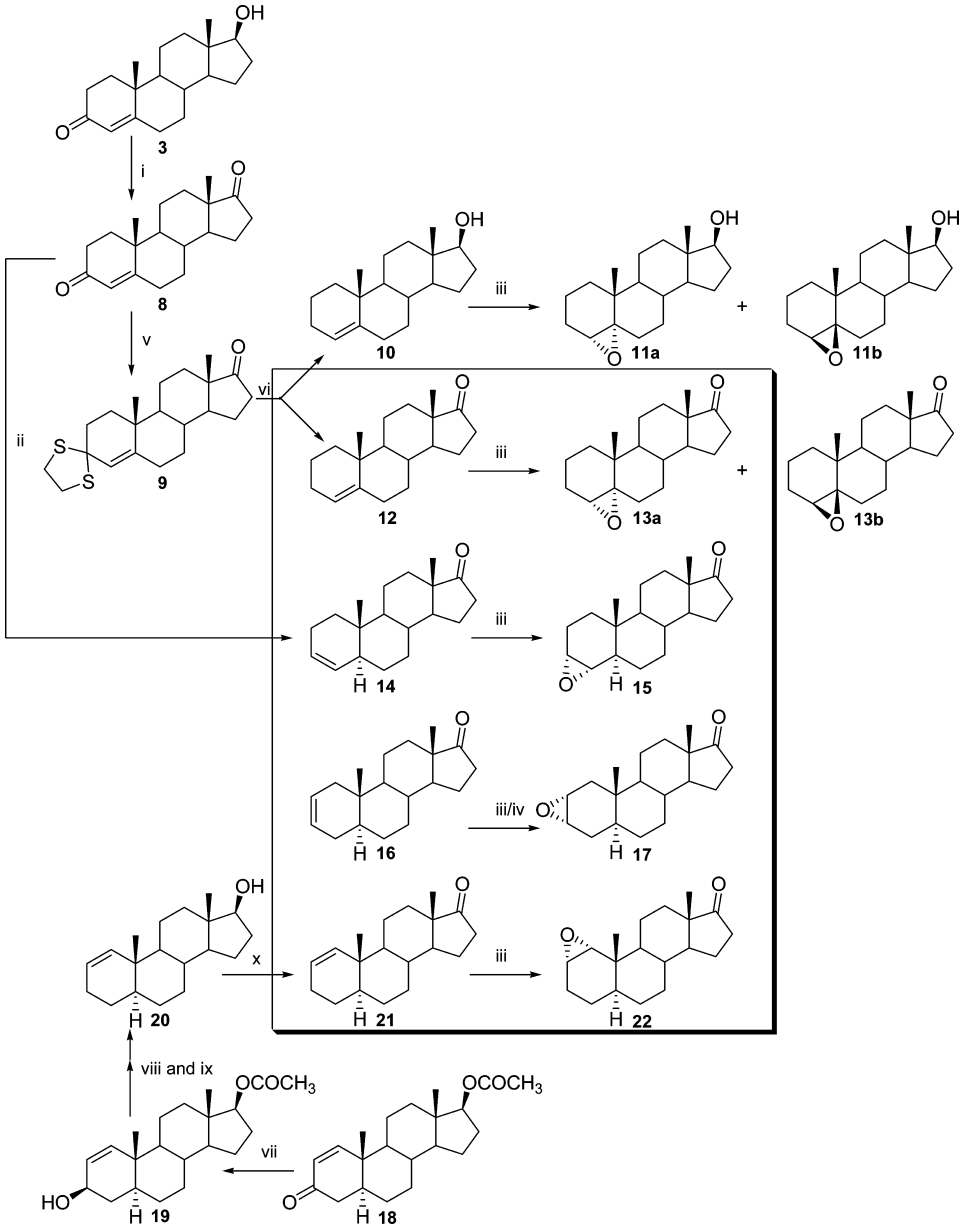

[a]Reagents and conditions: (i) CrO_3, H_2SO_4, acetone, rt; (ii) CH_3COOH, Zn dust, reflux, 15 min; (iii) H_2O_2, HCOOH, CH_2Cl_2, rt; (iv) CH_3COOOH, $CH_3COONa{\cdot}3H_2O$, $CHCl_3$, rt, 7 h 30 min; (v) $HSCH_2CH_2SH$, anhydrous *p*-toluenesulfonic acid, anhydrous THF, rt, 4 h 5 min; (vi) Na, NH_3, anhydrous THF, −65 °C, 25 min; (vii) (*t*-butoxi)$_3$AlLiH, anhydrous THF, reflux, 3h 15 min; (viii) $SOCl_2$, benzene, 5−8 °C, 3 h 15 min; (ix) $AlLiH_4$, diethyl ether, reflux, 10 h 30 min; (x) CrO_3, H_2SO_4, acetone, 0 °C.

crystallization gave compound **4** in 22% yield (Method B). Compound **3** was also converted to its 17β-acetate **6** in acetic anhydride in 84% yield (Scheme 1).[17] Compound **6** was then reduced by sodium borohydride, leading to a mixture of the 3β-**7** and 3α-epimers (90:10, respectively, NMR and HPLC). Attempts to isolate **7** by crystallization led, however, to enrichment of the mixture in the 3α-isomer. Compound **5** was obtained quantitatively from the commercially available compound **2**, by reducing this last compound with sodium borohydride in methanol, at room temperature (Scheme 1).

Compound **8** was prepared through the oxidation of **3** with Jones Reagent in 98% yield (Scheme 2).[12] Protection of the C-3 carbonyl group of **8** was undertaken by treatment with ethane-1,2-dithiol in anhydrous THF and in the presence of anhydrous *p*-toluenesulfonic acid.[18] The crude product obtained was purified by column chromatography affording the protected compound **9** in 84% yield and also the product resulting from the simultaneous protection of the C-3 and C-17 carbonyl groups, in 5% yield. Desulfurization of compound **9** with sodium-ammonia in anhydrous THF[19] afforded compound **12** in 46% yield and compound **10** in 26% yield. The crude material resulting from the treatment of compound **12**, in dichloromethane, with performic acid was purified by crystallization and column chromatography allowing the isolation of the main product of the reaction (one TLC spot). NMR analysis of this product revealed it to be a mixture of the isomers **13a** and **13b**, in 66:34 proportion. Further purification by column chromatography allowed the isolation of

dx.doi.org/10.1021/jm300262w | J. Med. Chem. 2012, 55, 3992−4002

Scheme 3. Synthesis of Aromatase Inhibitors from 23[a]

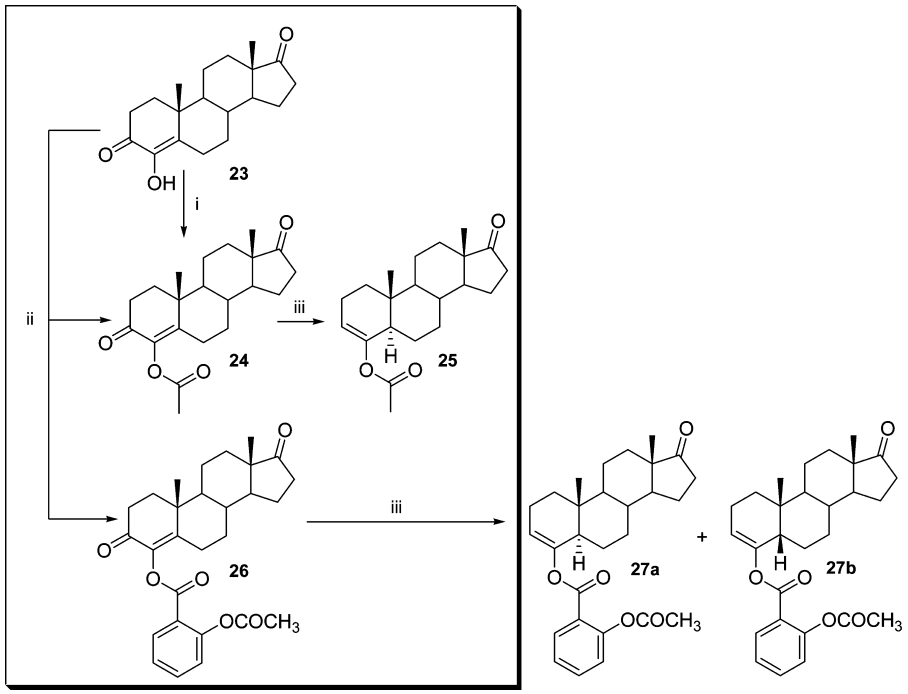

[a]Reagents and conditions: (i) acetyl chloride, dry pyridine, rt, 21 h 50 min; (ii) *o*-acetylsalicyloyl chloride, dry pyridine, rt, 24 h 40 min; (iii) Zn dust, CH_3COOH, rt.

Scheme 4. Synthesis of 28 from 14[a]

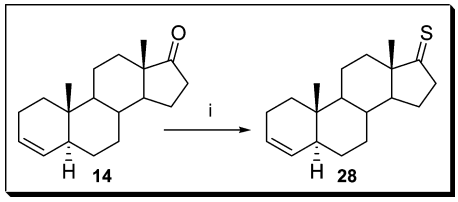

[a]Reagents and conditions: (i) Lawesson's reagent, dry toluene, reflux, 7 h.

the pure compound **13a** in 7.6% yield. Compound **10** was treated in the same way as compound **12**, allowing the isolation of the main product of the reaction, which after NMR analysis revealed itself to be a mixture of the two 4,5-epoxide isomers **11a** and **11b**, in a 60:40 proportion (Scheme 2). In agreement with a previous description of our group,[10] a Clemmenson-type reduction of **8** with zinc dust in acetic acid solution gave a mixture of 5α- and 5β-epimers from which the 5α-epimer **14** was isolated by *n*-hexane crystallization in 60% yield. Treatment of **14** with performic acid in dichloromethane led to the epoxide derivative **15**, in 96% yield (Scheme 2).[10] The 2,3-epoxide **17** was synthesized from the commercially available 2,3-olefin **16** by two different pathways: via performic acid, Method A,[12] and via peracetic acid, Method B.[20] As the starting material **16** was only available in 92% purity (it is supplied in a 92:8 inseparable mixture with **14**), the resulting compound **17** was also obtained in 92% purity (NMR and HPLC analysis) (Scheme 2), by both methods. 1,2-Olefin **21** was prepared following a described strategy.[17,21] Briefly, treatment of enone **18** with lithium tri-*t*-butoxyaluminum hydride gave the desired allylic alcohol **19** in 94% yield (Scheme 2). Compound **19** was then treated with thionyl chloride in benzene, under nitrogen. From this reaction, a complex mixture of products was obtained and used as starting material in the next reaction. Treatment of this mixture with lithium aluminum hydride led, after workup, to the main product **20** which after Jones oxidation afforded compound **21**. Treatment of **21** with a solution of performic acid in dichloromethane gave compound **22** in 15% yield.

Compound **23** was treated with acetyl chloride in dry pyridine leading, after crystallization, to the pure compound **24**, in 72% yield (Scheme 3). Compound **24** was treated with dust zinc in acetic acid solution leading to a mixture of both 5α- and 5β-epimers which after crystallization with petroleum ether allowed the isolation of the pure epimer **25**. Treatment of **23** with *o*-acetylsalicyloyl chloride in pyridine led, after purification by column chromatography, to a main fraction (one single TLC spot) which after NMR analysis was revealed to be composed by a mixture of compounds **24** and **26**, in 40:60 proportion. The formation of compound **24** probably resulted from an intramolecular transesterification occurring in **26**. Further purification by column chromatography using a different mixture of solvents allowed the isolation of the pure compound **26**. Treating **26** with zinc dust in acetic acid solution led to an inseparable epimeric mixture of the ester **27a** and its 5β-epimer **27b** in a 70:30 proportion (NMR analysis) (Scheme 3).

The synthesis of thione **28** was performed with Lawesson's reagent[22] and required an environment with controlled humidity. This reaction occurred within 7 h, although it was not complete. The reaction mixture was worked up with a prior elimination of Lawesson's reagent using an aluminum oxide neutral column. This additional step to the conventional workup was developed after observing that there was a reaction of Lawesson's reagent with silica gel leading to a complete decomposition of the product when the crude was directly chromatographed through a silica gel column. After reagent elimination, the crude product was purified by silica gel column

dx.doi.org/10.1021/jm300262w | J. Med. Chem. 2012, 55, 3992−4002

chromatography and afforded thione **28**, in 54% yield (Scheme 4).

Biochemistry. Inhibition of aromatase activity of the studied A- and D-ring modified steroids was evaluated in human placental microsomes by a radiometric assay in which tritiated water, released from [1β-^{3}H] androstenedione into the incubation medium, was used as an index of estrogen formation.[23] A screening assay was performed, and the results (Table 1) are shown as a percentage of inhibition (%) for all compounds at 2 μM, relative to an assay carried out in the absence of the inhibitor. AI **23** at 0.5 μM (99.65 ± 0.06%) was used as reference. For the steroids **1**, **12**, **13a**, **16**, and **17** with aromatase inhibition higher than 70%, the IC_{50} with a concentration of [1β-^{3}H] androstenedione of 100 nM (Table 2) was determined. For steroids **1**, **13a**, and **16**, kinetic studies to characterize the type of binding to the active site of the enzyme and the apparent inhibition constant (K_i) were also performed, using different concentrations of inhibitor and substrate (Table 2). These steroids were revealed to be competitive inhibitors. Representative Lineweaver–Burk and Dixon plots for compound **13a** are presented in Figures 2 and 3, respectively.

Table 1. Aromatase Inhibition of Tested Compounds at 2 μM in Human Placental Microsomes[a]

compds	aromatase inhibition (%) ± SEM
1	93.14 ± 2.36
2	60.84 ± 2.61
4	56.82 ± 5.59
5	6.59 ± 2.00
7	4.60 ± 0.40
12	97.84 ± 0.19
13a	84.59 ± 0.51
14[10,12]	95.90 ± 0.60
15[10,12]	96.40 ± 0.10
16	72.05 ± 2.60
17	70.70 ± 4.25
21	55.99 ± 1.86
22	40.01 ± 2.05
25	33.90 ± 1.68
26	68.73 ± 3.53
28	41.45 ± 2.05
formestane (**23**)	99.65 ± 0.06

[a]Concentrations of 40 nM [1β-^{3}H]androstenedione, 20 μg of protein from human placental microsomes, 2 μM of the compounds, and 15 min of incubation were used. The experiments were done in triplicate. The results represent the mean ± SEM of three different experiments. Compound **23** at 0.5 μM was used as reference.

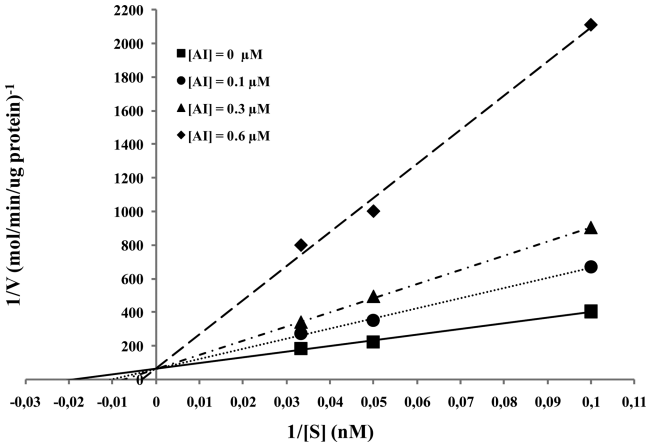

Figure 2. – Lineweaver–Burk plot of inhibitor **13a**. Different concentrations of inhibitor (0, 0.1, 0.3, and 0.6 μM), with **8** as substrate at 10, 20, and 30 nM, were used. Each point represents the mean of three independent determinations done in triplicate. The experiments with the other compounds gave similar plots to the results shown for **13a**.

DISCUSSION AND CONCLUSIONS

As referred to in the introduction, aromatase establishes two main hydrogen bonds with the carbonyl functions at C-3 and C-17 of its natural substrate **8**.[9] Nevertheless, it is known that the presence of the carbonyl group at C-3 is not mandatory to bind steroid molecules to the enzyme aromatase and to get aromatase inhibition.[10] The C-17 carbonyl group, however, seems to have a more important role in steroidal AIs. In any case, at least one of the referred carbonyl groups must exist in order to allow the binding of steroid molecules to the enzyme aromatase.[12] In this work, several steroid molecules were studied as AIs in which the carbonyl group at C-3 (a hydrogen bond acceptor) of **8** was replaced by a hydroxyl group (a hydrogen bond donor) and also in which the two carbonyl groups (C-3 and C-17) were replaced by two hydroxyl groups. Looking at compounds **1** and **2** (Scheme 1 and Table 1), we

Table 2. IC_{50} and Kinetic Studies for the Most Potent Inhibitors

compds	IC_{50} (μM)[a]	type of inhibition	kinetic studies[b] V_m (mol/min/μg prot)	Ki (μM)	real affinity (K_m/K_i) (nM)
1	0.183	competitive	0.225 ± 0.025	0.100	1.026 ± 0.026
12	0.135				
13a	0.970	competitive	0.015 ± 0.001	0.086	0.636 ± 0.058
14[10,12]	0.225	competitive		0.050	
15[10,12]	0.145	competitive		0.038	
16	1.733	competitive	0.200 ± 0.010	9.501	0.012 ± 0.002
17	1.150				
formestane (**23**)	0.042				

[a]Concentrations of 100 nM [1β-^{3}H]androstenedione, 20 μg protein from human placental microsomes, different concentrations of the compounds, and 15 min of incubation were used. [b]Concentrations of 10, 20, 30, and 40 nM [1β-^{3}H]androstenedione, 20 μg of protein from human placental microsomes, different concentrations of the compounds, and 5 min of incubation were used. Apparent inhibition constants (K_i) were obtained by Dixon Plot. Inhibition type was based on analysis of the Lineweaver–Burk plot. The experiments were done in triplicate in three independent experiments.

dx.doi.org/10.1021/jm300262w | J. Med. Chem. 2012, 55, 3992–4002

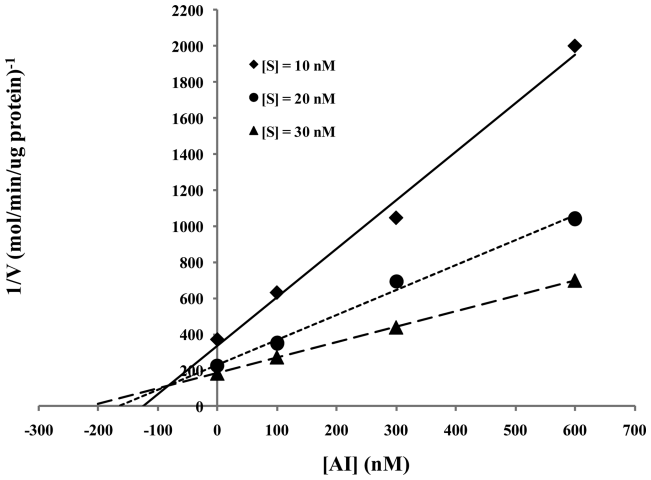

Figure 3. Dixon plot of inhibitor **13a**. Different concentrations of inhibitor (0, 0.1, 0.3, and 0.6 μM), with the substrate **8** at 10, 20, and 30 nM, to determine the apparent inhibition constant (K_i), were used. Each point represents the mean of three independent experiments done in triplicate. The experiments with the other compounds gave similar plots to the results shown for **13a**.

observed that the substitution of the C-3 carbonyl group of **8** by a C-3 hydroxyl group, maintaining the C-17 carbonyl group, led to a potent AI when the C-3-OH assumes the 3β stereochemistry. Compound **1** is in fact a very strong AI, with an IC_{50} of 0.18 μM, having also a high affinity to the enzyme (K_i of 0.1 μM) (Table 2). The C-3α-OH analogue **2** was not as good an AI as **1**. Changing the two carbonyl groups of **8**, at C-3 and C-17, by hydroxyl groups, a dramatic decrease in activity was observed (compounds **4** and **5**), particularly if the C-3-OH assumes the 3α stereochemistry (compound **5**) (Table 1). This decrease was also observed by the authors for other compounds submitted to the same transformation in C-17.[12] The lack of both C-3 and C-17 carbonyl groups in **4** and **5** can explain the inability of these steroids to bind conveniently to the enzyme with the consequent loss of activity. As the C-3-OH stereochemistry seems to play an interesting role in the aromatase inhibitory capacity of this kind of compound, a molecular docking study in the aromatase active site was done for compounds **1** and **2**. IFD simulations revealed the ability to establish one hydrogen bond between the C-17 carbonyl group and Met 374 (1.8 Å) by both compounds. Accordingly, the different aromatase recognition of **1** and **2** can be addressed to the hydrogen bond network of C-3-OH. In the former case, **1** donates and accepts two hydrogen bonds, respectively, with Thr 310 (2.1 Å) and Ile 305 (2.4 Å) (Figure 4), and in the latter case, **2** establishes only one hydrogen bond with Asp 309 (2.1 Å) (data not shown). Considering 100% of the volume of the aromatase binding site in the crystallographic model 3EQM, the IFD simulations with ligand **1** induced an increase of the cavity equal to 113%. Concerning compound **7** (Scheme 1), as expected the substitution of the C-17 hydroxyl group by the C-17 acetoxy group dramatically reduces the aromatase inhibitory activity (Table 1). The acetoxy group is, in fact, a bulky group and may cause steric hindrance at the enzyme active site. This is in accordance with previous studies of the authors[12] and is consistent with the short volume of the aromatase binding pocket, as recently described.[9]

As reported before, some planarity in the A-ring and in the A,B-ring junction has been revealed to be important for steroids

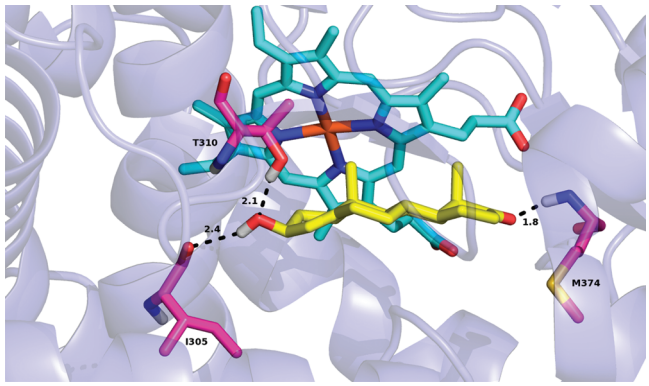

Figure 4. Best pose of inhibitor **1** within the aromatase binding pocket shown as a transparent cartoon. The ligand is represented as a yellow carbon polytube model. The heme and the labeled residues interacting via hydrogen bonds with **1** are, respectively, displayed by cyan and magenta carbon polytube models. Hydrogen bonds are depicted as dashed black lines, and their distances are measured in Å. Nonpolar hydrogen atoms are omitted for the sake of clarity.

having antiaromatase activity.[10,12] This planarity could be achieved introducing a double bond or an epoxide function into the A-ring, both possessing similar bond geometries. In this work, we are interested in studying the effect of the double bond or he epoxide function and its different positioning along the A-ring, in aromatase inhibitory activity. Considering the A-ring olefins (**12**, **14**, **16**, and **21**) and the corresponding epoxides (**13a**, **15**, **17** e **22**) (Scheme 2), it was observed that 4,5-olefin **12** and 1,2-olefin **21** are better AIs than the corresponding epoxides **13a** and **22**. Interestingly and on the contrary, the 3,4-epoxide **15** and the 2,3-epoxide **17** are better AIs than the corresponding olefins **14** and **16** (Tables 1 and 2). As published previously by the authors, for a similar 3,4-epoxide,[12] the oxiran oxygen in the 3,4 position may resemble the C-3 carbonyl oxygen of the aromatase substrate **8**, allowing it to establish hydrogen bonds with aromatase active site residues. IFD results also indicate **15** as being able to accept two hydrogen bonds with the aromatase. Notably, they are both established with the Thr 310 residue (Figure 5), in particular with the NH backbone (2.4 Å) and OH side chain (2.3 Å).

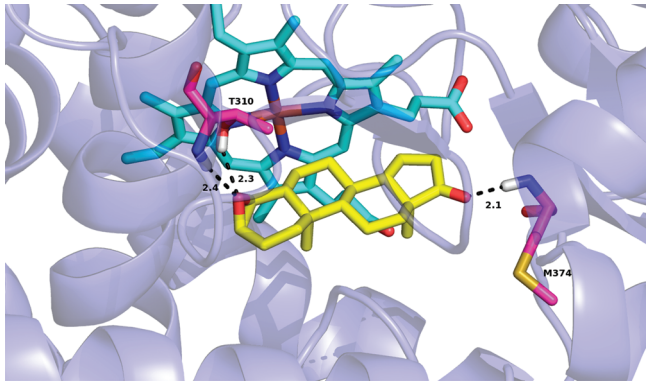

Figure 5. Best pose of inhibitor **15** within the aromatase binding pocket shown as a transparent cartoon. The ligand is represented as a yellow carbon polytube model. The heme and the labeled residues interacting via hydrogen bonds with **15** are, respectively, displayed by cyan and magenta carbon polytube models. Hydrogen bonds are depicted as dashed black lines, and their distances are measured in Å. Nonpolar hydrogen atoms are omitted for the sake of clarity.

dx.doi.org/10.1021/jm300262w | J. Med. Chem. 2012, 55, 3992−4002

Interestingly, in the lowest energy pose, inhibitor **15** fits the receptor core adopting an inverted non-canonical positioning when compared with aromatase substrate **8**, keeping the C-19 methyl group in the opposite side of the heme group (Figure 5). As observed for compound **1**, the volume of the binding site was quite affected by the presence of compound **15** with respect to **8**. The IFD simulations with ligand **15** induced a remarkable increase of the cavity equal to 123% (considering 100% the volume with the substrate **8**). The main reason can be attributed to the conformational change of Phe 221 and Trp 224 side chains, both located in the same aromatase α helix (Figure 6).

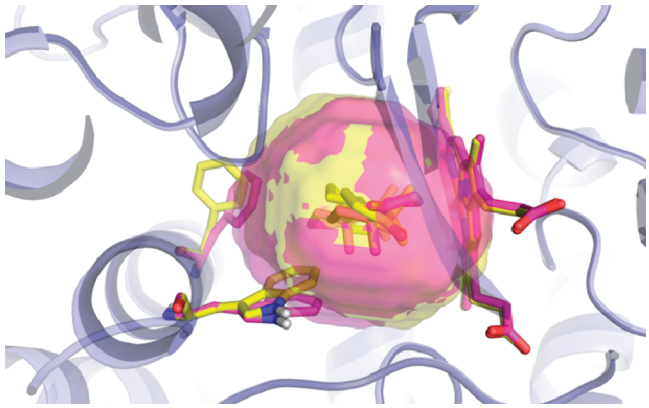

Figure 6. Aromatase binding site volume comparison between **1** and **15** induced fit models reported, respectively, in magenta and yellow colors. The ligands, the heme, and the most involved residues in the conformational change (Phe 221 and Trp 224) are displayed in polytube models. The rest of the protein is rendered as transparent cartoons. Nonpolar hydrogen atoms are omitted for the sake of clarity.

Another observation is related to the fact that when the double bond is closer to the A,B-ring junction in C-5, the highest aromatase inhibition is reached (Table 1), confirming that planarity in C-5 A,B-ring junction is very important to aromatase inhibition. Among the studied olefins and epoxides, compound **12**, which has a C-4 double bond, showed effectively the best aromatase inhibition. Numazawa et al. had already described this compound as a very strong AI.[24] Among the epoxides, compound **15** showed the best aromatase inhibitory activity (IC_{50} = 0.145 μM).

As pointed out in the Introduction, the C-4 acetoxy derivative **24** of the first steroidal AI clinically used, **23**, also revealed strong aromatase inhibitory activity.[13] On the basis of this, a new AI (compound **26**) based on **23** was designed and synthesized, by esterification of its C-4 hydroxyl group with the acetylsalicylic acid moiety (Scheme 3). Unfortunately, the C-4 acetylsalicyloxy derivative **26** showed a pronounced decrease in aromatase inhibition when compared with its precursor **23** (Table 1). The results obtained so far suggest that the presence of bulky substituents in C-4 diminishes the aromatase inhibitory activity, which is consistent with the short volume of the binding pocket of aromatase.[9] The C-4 acetoxy derivative **25** of olefin **14** also showed a dramatic reduction in the aromatase inhibitory activity, when compared with that of **14** (Table 1). In this case, the introduction of a C-4 acetoxy group did not maintain aromatase inhibitory activity, as observed in **24** relative to **23** (Scheme 3). Further, we assist reduction in the activity when we go from **24** to **25**, which is probably due to the displacement of the 4,5 double bond to the 3,4 position, reinforcing the importance of having planarity in the A,B-ring junction at C-5.

In Scheme 4, we present the synthesis of thione **28** from ketone **14**. Compound **28** was designed based on the isosterism concept by performing the chemical substitution of the C-17 carbonyl oxygen by the sulfur atom. It was observed that this transformation resulted in a loss of aromatase inhibitory activity, which prompted us to conclude that the sulfur atom was not as able as the oxygen atom to establish a hydrogen bond with the Met 374 residue, in the aromatase active site.

In summary, new AIs and new SARs have been found. Briefly, the β configuration of C-3 hydroxyl derivatives of aromatase substrate **8** is beneficial for aromatase inhibition; A-ring olefins are better inhibitors than the corresponding epoxides, except 2,3-epoxide **17** and 3,4-epoxide **15**, probably due to the possible establishment of additional hydrogen bonds with aromatase residues; planarity near the C-5 A,B-ring junction seems to be important for inhibitory activity since 4,5-olefin **12** is a better inhibitor than 3,4-olefin **14**, **14** is a better inhibitor than 2,3-olefin **16**, and **16** is a better inhibitor than 1,2-olefin **21**; and bulky substituents at C-4 and substitution of the C-17 carbonyl oxygen by the sulfur atom seem not to be beneficial for aromatase inhibition.

Although the new AIs found are not as potent as those already used as drugs, they showed some promising activities and can be studied for their effects in bone and in resistant cell lines in order to find molecules that can overcome the side effects and resistance shown by the drugs in clinical use.

EXPERIMENTAL SECTION

Chemistry. Melting points (mps) were determined on a Reichert Thermopan hot block apparatus and were not corrected. IR spectra were recorded on a Jasco 420FT/IR spectrometer. The ^{1}H NMR spectra were recorded at 600 MHz, on a Varian Unity 600. The ^{13}C NMR spectra were recorded at 150 MHz on a Varian Unity 600. Chemical shifts were recorded in δ values in parts per million (ppm) downfield from tetramethylsilane as an internal standard. All *J*-values are given in Hz. HRMS analyses were made on a QTof instrument from Applied Biosystems using the electrospray technique. Mass spectra ESI and LC-MS were obtained with a mass spectrometer QIT-MS Thermo Finningan, model LCQ Advantage MAX coupled to a Liquid Chromatograph of High Performance Thermo Finningan. 3β-Hydroxyandrost-4-en-17-one (**1**), 3α-hydroxyandrost-4-en-17-one (**2**), 5α-androst-2-en-17-one (**16**), and 3-oxo-5α-androst-1-en-17β-yl acetate (**18**) were purchased from Steraloids, Inc. (Newport RI, USA). Testosterone (**3**) was purchased from STEROID, (Cologno, Monzese, MI). Formestane (**23**) was purchased from Sigma-Aldrich, Inc. (St. Louis, USA). Reagents and solvents were used as obtained from the suppliers without further purification. Yields have not been optimized. Compounds **8**, **14**, and **15** were prepared as described.[12]

All compounds possess a purity superior to 95%, except compound **7** (90% purity) and compounds **16** and **17** (92% purity). The purity was checked by HPLC with a C18-reversed phase column and water/acetonitrile 40:60 as solvent. The purity of individual compounds was determined from the peak areas in the chromatogram of the sample solution.

Androst-4-ene-3β,17β-diol (4). *Method A.* To a solution of **3** (1.0 g, 3.47 mmol) in dry methanol (30.0 mL), sodium borohydride (350.1 mg, 9.25 mmol) was added, and the reaction was stirred at room temperature for 1 h 20 min, after which a supplement of 100 mg of sodium borohydride was added to completely transform the starting material (2 h 40 min, TLC). After methanol removal under vacuum, water (100 mL) was added and the product extracted with ethyl acetate (3× 200 mL). The organic layer was then washed with water (200 mL), dried over anhydrous $MgSO_4$, filtered, and

dx.doi.org/10.1021/jm300262w | J. Med. Chem. 2012, 55, 3992−4002

concentrated to dryness giving a white solid residue (1.04 g) composed by a mixture of **4** and its 3α-epimer **5**. Crystallization from methanol gave pure compound **4** (214.7 mg, 21%) as white crystalline plates. $Mp_{(methanol)}$ 149−151 °C. IR (NaCl plates, $CHCl_3$) υ_{max} cm^{-1}: 3361 (OH), 1656 (C═C), 1051 (C−O). ^1H (600 MHz, DMSO-d_6) δ: 0.64 (3H, s, 18-H_3), 0.98 (3H, s, 19-H_3), 3.41 (1H, ddd, $J_{17\alpha-16\alpha}$ = 8.5, $J_{17\alpha-16\beta}$ = 8.5, $J_{17\alpha\text{-}17\beta OH}$ = 4.5, 17α-H), 3.90 (1H, m, 3α-H), 4.44 (1H, d, $J_{17\beta OH\text{-}17\alpha}$ = 4.5, 17β−OH), 4.54 (1H, d, $J_{3\beta OH\text{-}3\alpha}$ = 5.4, 3β−OH), 5.17 (1H, bs, 4-H). ^{13}C (150 MHz, DMSO-d_6) δ: 11.2 (C-18), 18.5 (C-19), 20.2, 23.0, 29.0, 29.7, 31.5, 32.3, 35.3, 35.5, 36.4, 36.8, 42.4, 50.2, 54.2, 65.9 (C-3), 79.9 (C-17), 125.3 (C-4), 144.2 (C-5). ESI: 289.2 ($[M - H]^+$, 84%).

Method B. To a solution of **3** (1.0 g, 3.47 mmol) in dry tetrahydrofuran (40.0 mL), lithium tri-*t*-butoxyaluminium hydride (1.15 g, 4.51 mmol) was added, and the reaction was heated under reflux for 2 h 30 min. To completely transform the starting material (TLC), 874 mg of tri-*t*-butoxyaluminum hydride was added in several portions and the reaction stirred at room temperature for a further 8 h 20 min. After methanol removal under vacuum, water (100 mL) was added and the product extracted with ethyl acetate (3 × 200 mL). The organic layer was then washed with water (200 mL), dried over anhydrous $MgSO_4$, filtered, and concentrated to dryness giving a white solid residue (1.04 g) composed by a mixture of **4** and **5**. Crystallization from methanol gave the pure compound **4** (222.1 mg, 22%) as white crystalline plates.

Androst-4-ene-3α,17β-diol (5). To a solution of **2** (10 mg, 0.035 mmol) in methanol (3 mL), sodium borohydride (4.64 mg, 0.123 mmol) was added, and the reaction mixture was stirred at room temperature until all of the starting material had been consumed (10 min, TLC). After methanol evaporation and dissolution of the residue obtained with ethyl acetate (50 mL), the organic layer was washed with water (3 × 40 mL), dried over anhydrous $MgSO_4$, filtered, and evaporated affording pure compound **5**, in quantitative yield as a white residue. $Mp_{(dichloromethane/methanol)}$ 202−205 °C. IR (KBr) ν_{max} cm^{-1}: 3328 (OH), 1655 (C═C), 1054 (C−O). ^1H NMR (600 MHz, DMSO-d_6) δ: 0.66 (3H, s, 18-H_3), 0.92 (3H, s, 19-H_3), 3.41−3.45 (1H, m, 17α-H), 3.85 (1H, bs, 3-H), 4.29 (1H, d, J = 4.8, 3α−OH or 17β−OH), 4.38 (1H,d, J = 4.8, 3α−OH or 17β−OH), 5.30 (1H, s, J = 4.2, 4-H). ^{13}C NMR (150 MHz, DMSO-d_6) δ: 11.1 (C-18), 18.0 (C-19), 20.7, 23.0, 27.7, 29.7, 31.3, 31.6, 32.1, 35.4, 36.5, 36.9, 40.0, 42.4, 50.3, 53.2, 62.3 (C-3), 79.9 (C-17), 122.2 (C-4). ESI: 289.5 ($[M - H]^+$, 100%).

3β-Hydroxyandrost-4-en-17β-yl Acetate (7). To a solution of **6** (676.5 mg, 2.04 mmol) in dry methanol (20 mL), sodium borohydride (127.5 mg, 3.37 mmol) was added, and the reaction was stirred at room temperature until complete transformation of the starting material (45 min, TLC). After removal of methanol under vacuum, water (200 mL) was added and the product extracted with ethyl acetate (3 × 200 mL). The organic layer was washed with water (200 mL), dried over anhydrous $MgSO_4$, filtered, and concentrated to dryness giving a white solid residue (706.4 mg). This residue was purified by a silica gel 60 column chromatography (petroleum ether 60−80 °C/ethyl acetate) affording 430.0 mg of a 90:10 3β/3α-epimeric mixture of 3-hydroxyandrost-4-en-17β-yl acetate (NMR and HPLC control). An attempt to isolate 3β-epimer **7** by crystallization just enriched the mixture in the 3α-epimer. 3β-Hydroxyandrost-4-en-17β-yl acetate (**7**): ^1H NMR (600 MHz, DMSO-d_6) δ, 0.76 (3H, s, 18-H_3), 0.99 (3H, s, 19-H_3), 1.98 (3H, s, CH_3COO), 3.90 (1H, m, 3α-H), 4.49 (1H, dd, $J_{17\alpha-16\alpha}$ = 9.0, $J_{17\alpha H\text{-}16\beta H}$ = 8.0, 17α-H), 4.54 (1H, d, $J_{3\beta OH\text{-}3\alpha}$ = 5.5, 3β−OH), 5.19 (1H, bs, 4-H). ^{13}C NMR (150 MHz, DMSO-d_6) δ: 11.8 (C-18), 18.4 (C-19), 20.0, 20.8, 22.9, 27.0, 28.9, 31.4, 32.2, 35.1, 35.2, 36.2, 36.7, 41.9, 49.7, 53.8, 65.8 (C-3), 81.8 (C-17), 125.5 (C-4), 143.9 (C5), 170.2 (OC═O). ESI: 331.0 ($[M - H]^+$, 100%). 3α-Hydroxyandrost-4-en-17β-yl acetate: ^1H NMR (600 MHz, DMSO-d_6) δ, 0.77 (1H, s, 18-H_3), 0.92 (1H, s, 19-H_3), 1.98 (3H, s, CH_3COO), 3.85 (1H, m, 3β-H), 4.36 (1H, d, $J_{3\alpha OH\text{-}3\beta}$ = 4.4, 3α−OH), 4.50 (1H, dd, $J_{17\alpha\text{-}16\alpha}$ = 9.0, $J_{17\alpha\text{-}16\beta}$ = 8.0, 17α-H), 5.31 (1H, d, $J_{4-3\beta}$ = 4.5, 4-H).

General Procedure to Obtain 4α,5α- and 4β,5β-Epoxyandrostan-17β-ol (11a and 11b), 4α,5α-Epoxyandrostan-17-one (13a), 2α,3α-Epoxy-5α-androstan-17-one (17), and 1α,2α-Epoxyandrostan-17-one (22). To a solution of olefin (**10**, **12**, **16**, or **21**) in dichloromethane, a solution of performic acid, generated in situ by addition of 98−100% HCOOH to 35% H_2O_2, was added. The reaction mixture was stirred at room temperature until complete transformation of the starting material. Dichloromethane (100 mL) was added, and the organic layer was washed successively with 10% aqueous $NaHCO_3$ (2 × 100 mL) and water (4 × 100 mL), dried over anhydrous $MgSO_4$, filtered, and concentrated to dryness. The obtained residue was purified by silica gel 60 column chromatography (*n*-hexane/ethyl acetate).

4α,5α- and 4β,5β-Epoxyandrostan-17β-ol (11a and 11b). Olefin **10** (82.7 mg, 0.30 mmol); dichloromethane (4.0 mL); 98−100% HCOOH (0.04 mL); and 35% H_2O_2 (0.11 mL) were used; total reaction time, 7 h (TLC). Before column chromatography, 83.6 mg of a white solid residue was obtained. Purification by column chromatography afforded 39.7 mg of an inseparable epimeric mixture (60:40, by NMR) of **11a** and **11b**. 4α,5α-Epoxyandrostan-17β-ol (**11a**): ^1H NMR (600 MHz, DMSO-d_6) δ, 0.65 (3H, s, 18-H_3), 1.02 (3H, s, 19-H_3), 3.42−3.46 (1H, m, 17α-H), 2.86 (1H, d, $J_{4\beta\text{-}3\alpha}$ = 4.3, 4β-H), 4.42 (1H, d, $J_{17\beta OH\text{-}17\alpha}$ = 4.8, 17β−OH). 4β,5β-Epoxyandrostan-17β-ol (**11b**): ^1H NMR (600 MHz, DMSO-d_6) δ, 0.64 (3H, s, 18-H_3), 0.93 (3H, s, 19-H_3), 3.42−3.46 (1H, m, 17α-H), 2.86 (1H, d, $J_{4\alpha\text{-}3\alpha}$ = 4.6, 4α-H), 4.44 (1H, d, $J_{17\beta OH\text{-}17\alpha}$ = 4.9, 17β−OH).

4α,5α-Epoxyandrostan-17-one (13a). Olefin **12** (140.7 mg, 0.52 mmol); dichloromethane (4.0 mL); 98−100% HCOOH (0.07 mL); and 35% H_2O_2 (0.19 mL) were used; total reaction time, 6 h 30 min (TLC). Before column chromatography 141.9 mg of a white solid residue was obtained. Purification by column chromatography afforded 76.6 mg of the 4,5-epoxyandrostan-17-one in a mixture (66:34 by NMR) of 4α,5α- and 4β,5β-epimers **13a** and **13b**. Further purification by column chromatography with chloroform allowed us to isolate 11.4 mg (7.6%) of the pure 4α,5α-epimer **13a**. 4α,5α-Epoxyandrostan-17-one (**13a**): $mp_{(chloroform)}$ 142−145 °C. IR (NaCl plates, $CHCl_3$) ν_{max} cm^{-1}: 1734 (C═O), 1216 (C−O−C). ^1H NMR (600 MHz, $CDCl_3$) δ: 0.88 (3H, s, 18-H_3), 1.03 (3H, s, 19-H_3), 2.46 (1H, ddd, $J_{16\beta\text{-}16\alpha}$ = 19.0, $J_{16\beta\text{-}15\beta}$ = 9.0, $J_{16\beta\text{-}15\beta}$ = 1.0, 16β-H), 2.90 (1H, d, $J_{4\beta\text{-}3\alpha}$ = 4.6, 4β-H). ^{13}C NMR (150 MHz, $CDCl_3$) δ: 13.7 (C-18), 15.3 (C-19), 19.2, 20.5, 21.8, 23.6, 29.3, 29.6, 31.2, 31.4, 34.7, 35.8, 36.4, 46.7, 47.7, 51.2, 61.3, 65.3 (C-5), 220.9 (C-17). ESI: 287.1 ($[M - H]^+$, 100%). 4β,5β-Epoxy-androstan-17-one (from the mixture of **13a** + **13b**): ^1H NMR (600 MHz, $CDCl_3$) δ, 0.88 (3H, s, 18-H_3), 1.08 (3H, s, 19-H_3), 2.43 (1H, ddd, $J_{16\beta\text{-}16\alpha}$ = 19.0, $J_{16\beta\text{-}15\beta}$ = 9.0, $J_{16\beta\text{-}15\beta}$ = 1.0, 16β-H), 2.94 (1H, d, $J_{4\alpha\text{-}3\beta}$ =4.1, 4α-H).

2α,3α-Epoxy-5α-androstan-17-one (17). *Method A.* Olefin **16** (100 mg, 0.37 mmol); dichloromethane (2.0 mL); 98−100% HCOOH (0.1 mL); and 35% H_2O_2 (0.3 mL) were used; total reaction time, 6 h (TLC). Before column chromatography, 103.5 mg of a white solid residue was obtained. Purification by column chromatography (chloroform) afforded compound **17** (6.7 mg, 6%) in 92% purity (NMR and HPLC analysis). IR υ_{max} (NaCl plates $CHCl_3$) cm^{-1}: 1738(C═O), 1013 (C−O−C). ^1H NMR (600 MHz, $CDCl_3$) δ: 0.78 (3H, s, 19-H_3), 0.84 (3H, s, 18-H_3), 2.05 (1H, ddd, $J_{16\alpha\text{-}16\beta}$ = 19.0, $J_{16\alpha\text{-}15\beta}$ = 9.0, $J_{16\alpha\text{-}15\alpha}$ = 9.0, 16α-H), 2.42 (1H, ddd, $J_{16\beta\text{-}16\alpha}$ = 19.0, $J_{16\beta\text{-}15\beta}$ = 9.0, $J_{16\beta\text{-}15\alpha}$ = 1.0, 16β-H), 3.11 (1H, m, $J_{2\beta\text{-}1\alpha}$ = 6.0, $J_{2\beta\text{-}3\beta}$ = 3.95, 2β-H) and 3.16 (1H, m, $J_{3\beta\text{-}4\alpha}$ =6.0, $J_{3\beta\text{-}2\beta}$ = 3.95, $J_{3\beta\text{-}4\beta}$ = 1.69, 3β-H). ^{13}C NMR (150 MHz, $CDCl_3$) δ: 15.6 (C-19), 16.3 (C-18), 22.8, 24.4, 30.7, 31.6, 33.1, 34.1, 36.4, 37.8, 38.5, 38.9, 40.9, 50.2, 53.5, 53.9, 55.0 (C-2), 56.4 (C-3) and 223.9 (C-17). ESI: 287.0 ($[M - H]^+$, 100%).

Method B. To a stirred 9% aqueous peracetic acid solution (1.0 mL) at 10 °C, trihidrated sodium acetate (79.6 mg) and olefin **16** (200.2 mg, 0.73 mmol) in chloroform (2 mL) were added. The reaction was then stirred at room temperature until complete transformation of the starting material (7 h 30 min, TLC). Dichloromethane (150 mL) was added, and the organic layer was washed with 10% aqueous $NaHCO_3$ (100 mL), water (4 × 100 mL),

dx.doi.org/10.1021/jm300262w | *J. Med. Chem.* 2012, 55, 3992−4002

dried over anhydrous $MgSO_4$, and concentrated to dryness giving 162.9 mg of a white residue. Purification of this residue by the usual procedure gave compound **17**, also in 92% purity.

1α,2α-Epoxyandrostan-17-one (22). Olefin **21** (46.4 mg, 0.17 mmol); dichloromethane (3 mL); 98−100% HCOOH (0.03 mL); and 35% H_2O_2 (0.07 mL) were used; total reaction time, 9 h 30 min (TLC). Before column chromatography, 38.6 mg of an oily residue was obtained. Purification by column chromatography afforded 7.4 mg (15%) of the pure compound **22**. $Mp_{(chloroform)}$ 119−122 °C. IR (NaCl plates, $CHCl_3$) υ_{max} cm^{-1}: 1738 (C═O), 1049 (C−O). ^1H NMR (600 MHz, $CDCl_3$) δ: 0.87 (3H, s, 18-H_3), 0,92 (3H, s, 19-H_3), 2.07 (1H,ddd, $J_{16\alpha\text{-}16\beta}$ = 19.0, $J_{16\alpha\text{-}15\alpha}$ = 9.0, $J_{16\alpha\text{-}15\beta}$ = 9.0, 16α-H), 2.42 (1H, ddd, $J_{16\beta\text{-}16\alpha}$ = 19.0, $J_{16\beta\text{-}15\beta}$ = 9.0, $J_{16\beta\text{-}15\alpha}$ = 1.0, 16β-H), 2.99 (1H, d, $J_{1\beta\text{-}2\beta}$ = 4.0, 1β-H), 3.12 (1H, dd, $J_{2\beta\text{-}1\beta}$ = 4.0, $J_{2\beta\text{-}3\alpha}$ = 3.0, 2β-H). ^{13}C NMR (150 MHz, $CDCl_3$) δ: 11.4 (C-18), 13.8 (C-19), 20.4, 21.7, 22.7, 23.4, 27.6, 30.4, 31.3, 34.9, 35.8, 36.6, 37.3, 47.7, 49.0, 51.3, 52.9 (C-1), 59.1 (C-2), 221.1 (C═O). ESI: 286.9 ($[M - H]^+$, 100%).

4-Acetoxyandrost-4-en-3,17-dione (24). To a solution of **23** (750.6 mg, 2.48 mmol) in dry pyridine (12.5 mL), at 0 °C, acetyl chloride (0.27 mL, 3.80 mmol) was added dropwise. The reaction was stirred for 15 min at 0 °C, and then the temperature was raised to the ambient. Three subsequent additions of acetyl choride (3 × 0.1 mL) were made allowing the reaction to be complete (total reaction time: 21 h 50 min, TLC). The solvent was then evaporated under vacuum, and the obtained residue was crystallized with ethyl acetate/*n*-hexane after activated charcoal decoloration giving the pure compound **24** as white crystals (616.1 mg, 72%). $Mp_{(chloroform)}$ 169−171 °C. IR (NaCl plates, $CHCl_3$) ν_{max} cm^{-1}: 3018 (═CH), 1739 (C═O), 1680 (C═C), 1059 (C−O). ^1H NMR (600 MHz, $CDCl_3$) δ: 0.91 (3H, s, 18-H_3), 1.26 (3H, s, 19-H_3), 2.23 (3H, s, CH_3COO). ^{13}C NMR (150 MHz, $CDCl_3$) δ: 13.7 (C-18), 17.6 (C-19), 20.2, 20.3, 21.7, 23.9, 29.7, 31.2, 33.3, 34.6, 34.7, 35.7, 39.1, 47.4, 50.7, 53.8, 139.2, 154.9, 168.6, 190.4 (C-3), 220.2 (C-17).

4-Acetoxy-5α-androst-3-en-17-one (25). To a solution of **24** (90.3 mg, 0.26 mmol) in glacial acetic acid (7.5 mL), zinc dust (500.0 mg, 7.65 mmol) was added. The reaction was sonicated in an ultrasound bath at room temperature for 25 min, after which an excess of dust zinc (500.0 mg, 7.65 mmol) was added, and the reaction proceeded until all of the starting material had been consumed (2 h, TLC). Zinc was then filtered and washed with diethyl ether (50 mL), and the filtrate was concentrated under vacuum. To the oily residue obtained, water (100 mL) was added, and the product was extracted with dichloromethane (3 × 100 mL). The organic phase was sequentially washed with 10% aqueous $NaHCO_3$ (2 × 100 mL) and water (3 × 100 mL), dried over anhydrous $MgSO_4$, filtered, and concentrated to dryness giving an oily residue (105.9 mg) composed by a mixture of 4-acetoxy-5α-androst-3-en-17-one **25** and its 5β-epimer. Further crystallization with petroleum ether afforded the pure compound **25**, as white crystals. $Mp_{(petroleum\ ether)}$ 116−119 °C. IR (NaCl plates, $CHCl_3$) ν_{max} cm^{-1}: 3018 (═CH), 1737 (C═O), 1681 (C═C), 1158 (C−O). ^1H NMR (600 MHz, $CDCl_3$) δ: 0.86 (3H, s, 18-H_3), 0.88 (3H, s, 19-H_3), 2.11 (3H, s, CH_3COO), 5.24 (1H, dd, $J_{3-2\beta}$ = 6.6, $J_{3-2\alpha}$ = 3.3, 3-H). ^{13}C NMR (150 MHz, $CDCl_3$) δ: 12.4 (C-18), 13.9 (C-19), 20.5, 20.6, 20.7, 21.4, 21.7, 30.1, 31.5, 33.4, 34.7, 35.8, 36.5, 47.0, 47.8, 51.3, 53.0, 112.5 (C-3), 148.8 (C-4), 169.7, 221.0 (C-17). HRMS: *m/z* $[M + Na]^+$ calcd for $C_{21}H_{30}O_3$, 353.2087; found, 353.2080.

4-(*o*-Acetylsalicyloxy)androst-4-en-3,17-dione (26). To a solution of **23** (500.2 mg, 1.65 mmol) in dry pyridine (6.5 mL) at 0 °C, *o*-acetylsalicyloyl chloride (492.0 mg, 2.48 mmol) was added. The reaction mixture was stirred at room temperature for 22 h 30 min, and after that, an excess of *o*-acetylsalicyloyl chloride (247.4 mg, 1.25 mmol) was added. The reaction proceeded until complete transformation of the starting material (24 h 40 min, TLC). After evaporation of the solvent under vacuum, the residue was dissolved in dichloromethane (100 mL), and the organic layer was sequentially washed with 0.25 N aqueous HCl (4 × 100 mL), 10% aqueous $NaHCO_3$ (2 × 100 mL), and water (2 × 100 mL), dried over anhydrous $MgSO_4$, filtered, and concentrated to dryness giving a yellow oily residue (865.8 mg). This residue was then purified by silica gel 60 column chromatography (petroleum ether 40−60 °C/ethyl acetate) allowing us to separate 610.6 mg of compound **26** in a mixture with compound **24** (60:40 respectively, NMR). A portion of this mixture (127.7 mg) was further purified by further silica gel 60 column chromatography (*n*-hexane/diethyl ether) allowing us to isolate pure compound **26** (51.2 mg) as a white crystalline residue. $Mp_{(diethyl\ ether/n\text{-}hexane)}$ 183−185 °C. IR (KBr disk) υ_{max} cm^{-1}: 3453 (CH_{Ar}), 1769 (C═O ester), 1739 (C═O), 1687 (C═C), 1606 (C═C_{Ar}), 1195 (C−O). ^1H NMR (600 MHz, $CDCl_3$) δ: 0.92 (3H, s, 18-H_3), 1.32 (3H, s, 19-H_3), 2.28 (3H, s, CH_3COO), 7.12 (1H, d, J_{4-3} = 7.8, 4-H_{Ar}), 7.32 (1H, dd, J_{3-4} = 7.8, J_{3-2} = 7.8, 3-H_{Ar}), 7.57 (1H, dd, J_{2-3} = 7.8, J_{2-1} = 9.2, 2-H_{Ar}), 8.13 (1H, d, J_{1-2} = 9.2, 1-H_{Ar}). ^{13}C NMR (150 MHz, $CDCl_3$) δ: 13.7 (C-18), 17.8 (C-19), 20.4, 20.9, 21.7, 24.0, 29.9, 31.5, 33.4, 34.8, 34.9, 35.7, 39.4, 47.4, 50.9, 54.0, 122.8, 123.8 (C_{Ar}-4), 125.9 (C_{Ar}-3), 132.2 (C_{Ar}-2), 134.0 (C_{Ar}-1), 139.2, 151.1, 155.3, 162.1, 169.3, 189.8 (C-3), 219.5 (C-17). ESI: 463.7 ($[M - H]^+$, 100%).

4-(*o*-Acetylsalicyloxy)-5α-androst-3-en-17-one (27). A solution of a crude containing compound **26** as the main product (272.9 mg) in glacial acetic acid (25 mL) was sonicated with an ultrasound probe in the presence of excess of dust zinc (<10 μm) (4.73 g, 17.43 mmol) until the transformation of all of the starting material (20 min, TLC). Zinc was filtered and washed with glacial acetic acid, and then the filtrate was concentrated under vacuum. To the oily residue, water (200 mL) was added, and the product was extracted with dichloromethane (3 × 100 mL). The organic phase was sequentially washed with 10% aqueous $NaHCO_3$ (2 × 150 mL) and water (3 × 150 mL), dried over anhydrous Na_2SO_4, filtered, and concentrated to dryness giving an oily residue (242.9 mg). This residue was purified by a silica gel 60 column chromatography (petroleum ether 40−60 °C/ethyl acetate) allowing us to isolate 101.1 mg of 4-(*o*-acetylsalicyloxy)-5α-androst-3-en-17-one **27a** in an inseparable mixture with its 5β-epimer **27b** (70:30, respectively, by NMR). 4-(*o*-Acetylsalicyloxy)-5α-androst-3-en-17-one (**27a**): ^1H NMR (600 MHz, $CDCl_3$) δ, 0.87 (3H, s, 18-H_3), 0.93 (3H, s, 19-H_3), 2.33 (3H, s, CH_3COO), 5.36 (1H, dd, $J_{3-2\beta}$ = 6.6, $J_{3-2\alpha}$ = 3.3, 3-H), 7.12 (1H, d, J_{4-3} = 8.7, 4-H_{Ar}), 7.33 (1H, dd, J_{3-4} = 8.7, J_{3-2} = 8.7, 3-H_{Ar}), 7.58 (1H, dd, J_{2-3} = 8.7, J_{2-1} = 9.6, 2-H_{Ar}), 8.07 (1H, d, J_{1-2} = 9.6, 1-H_{Ar}). 4-(*o*-Acetylsalicyloxy)-5β-androst-3-en-17-one (**27b**): ^1H NMR (600 MHz, $CDCl_3$) δ, 0.87 (3H, s, 18-H_3), 1.05 (3H, s, 19-H_3), 2.34 (3H, s, CH_3COO), 5.51 (1H, dd, $J_{3-2\beta}$ = 6.9, $J_{3-2\alpha}$ = 3.6, 3-H), 7.12 (1H, d, J_{4-3} = 8.7, 4-H_{Ar}), 7.33 (1H, dd, J_{3-4} = 8.7, J_{3-2} = 8.7, 3-H_{Ar}), 7.58 (1H, dd, J_{2-3} = 8.7, J_{2-1} = 9.6, 2-H_{Ar}), 8.05 (1H, d, J_{1-2} = 9.6, 1-H_{Ar}).

5α-Androst-3-ene-17-thione (28). To a solution of olefin **14** (420.7 mg, 1.46 mmol) in dry toluene (30 mL), Lawesson's reagent (624.9 mg, 1.54 mmol) was added, and the reaction mixture was heated under reflux for 7 h, in an inert atmosphere. The remaining Lawesson's reagent was removed through an aluminum oxide neutral column leading to an orange residue, which was further purified by silica gel 60 column chromatography (petroleum ether 40−60 °C) affording pure compound **28** (238.5 mg, 54%), as a light orange solid. $Mp_{(petroleum\ ether\ 40-60\ °C)}$ 95 °C. IR (NaCl plates, $CHCl_3$) υ_{max} cm^{-1}: 3015 (═CH), 1650 (C═C), absence of C═O (peak around 1715 in compound **14**). ^1H NMR (600 MHz, $CDCl_3$) δ: 0.79 (3H, s, 19-H_3), 0.88 (3H, s, 18-H_3), 2.60 (1H, ddd, $J_{16\alpha\text{-}16\beta}$ = 22.0, $J_{16\alpha\text{-}15\beta}$ = 9.0, $J_{16\alpha\text{-}15\alpha}$ = 9.0, 16α-H), 2.93 (1H, ddd, $J_{16\beta\text{-}16\alpha}$ = 22.0, $J_{16\beta\text{-}15\beta}$ = 9.0, $J_{16\beta\text{-}15\alpha}$ = 1.0, 16β-H), 5.27 (1 H, ddd, J_{4-3} = 9.5, $J_{4-5\alpha}$ = 4.0, $J_{4-2\alpha}$ = 2.0, 4-H), 5.54 (1 H, ddd, J_{3-4} = 9.5, $J_{3-2\beta}$ = 6.0, $J_{3-2\alpha}$ = 3.0, 3-H). ^{13}C NMR (150 MHz, $CDCl_3$) δ: 14.5 (C-19), 20.5 (C-18), 23.7, 26.1, 27.1, 29.9, 34.3, 36.7, 37.7, 38.3, 38.6, 48.5, 51.8, 55.7 (2 carbons), 62.1, 128.2 (C-4), 133.7 (C-3), 274.1 (C═S). ESI: 287.2 ($[M - H]^+$, 100%).

Biochemistry. *Preparation of Placental Microsomes.* Placental microsomes were obtained as described by Yoshida and Osawa,[25] with some modifications as reported previously by our group.[10] Human placentas, obtained after delivery from a local hospital, were placed in cold 67 mM potassium phosphate buffer (pH 7.4) containing 1% KCl. The cotyledon tissue was separated and homogenized in a Polytron homogenizer with 67 mM potassium phosphate buffer (pH 7.4) containing 0.25 M sucrose and 0.5 mM dithiothreitol (DTT, 1:1, w/v). The

dx.doi.org/10.1021/jm300262w | J. Med. Chem. 2012, 55, 3992−4002

homogenate was centrifuged at 5000*g* for 30 min, and the supernatant was centrifuged at 20,000*g* for 30 min, and afterward at 54,000*g* for 45 min to yield the microsomal pellet. The microsomes were washed and ressuspended in 67 mM potassium phosphate buffer (pH 7.4) containing 0.25 M sucrose, 20% glycerol, and 0.5 mM DTT and stored at −80 °C. All procedures were carried out at 0−5 °C. Protein content was estimated by the Bio-Rad protein assay (Bio-Rad Laboratories, Munich, Germany) using BSA as a standard.

Aromatase Assay Procedure. Aromatase activity was measured according to Thompson and Siiteri,[23] and Heidrich et al.,[26] by measuring the tritiated H_2O released from [1β-^{3}H] androstenedione (PerkinElmer Life Sciences, Boston, MA, USA), during the aromatization process. All tested compounds were dissolved in DMSO and diluted in 67 mM potassium phosphate buffer (pH 7.4). Briefly, for the screening assay, (1 mL) 20 μg of protein of the microsomes, 40 nM of [1β-^{3}H] androstenedione (1 μCi), and 2 μM of each of the AIs were used for the reaction mixture. The aromatase-catalyzed reaction was initiated by the addition of NADPH (150 μM), and incubations were performed in a shaking water bath at 37 °C for 15 min. For the IC_{50} determination, 100 nM (1 μCi) of [1β-^{3}H] androstenedione and different concentrations of the inhibitors were used. For the kinetic studies and to minimize the time-dependent loss of the initial aromatization rate, 5 min of incubation time was used, and assays were performed with different concentrations of [1β-^{3}H] androstenedione (10−40 nM). All of the aromatase reactions were terminated by the addition of 250 μL of 20% trichloroacetic acid. The mixture was transferred to microcentrifuge tubes containing a charcoal−dextran pellet, vortexed, and incubated for 1 h. After centrifugation at 14,000*g* for 10 min, the supernatants were transferred to new charcoal−dextran pellets, incubated for 10 min, and subsequently pelleted by a new centrifugation cycle. The supernatant containing the tritiated water product was mixed with a liquid scintillation cocktail (ICN Radiochemicals, Irvine, CA, USA) and counted in a liquid scintillation counter (LS-6500, Beckman Coulter, Inc., Fullerton, CA). All experiments were carried out in triplicate.

Docking Experiments. The X-ray coordinates of human aromatase in complex with its substrate **8** were extracted from the PDB (code 3EQM).[9] Initially, both ligand and enzyme were pretreated. For ligand preparation, the 3D structures of all the studied compounds were generated with the Maestro Build Panel. The target structure was prepared through the Protein Preparation Wizard of the graphical user interface Maestro 9.1[27] and the OPLS-2005 force field.[28] All water molecules were removed, hydrogen atoms were added, and, finally, energy minimization was performed until the rmsd of all heavy atoms was within 0.3 Å of the original PDB model.

Docking studies were carried out using IFD.[14] An initial Glide SP docking of each ligand was performed by using a softened potential, a van der Waals radius scaling factor of 0.50 for receptor/ligand atoms, and a number of 20 poses per ligand to be energy minimized with the OPLS-AA force field.[29] The poses were saved for each ligand and submitted to the subsequent Prime side chain orientation prediction of residues with a distance cutoff of 5 Å around each ligand. After the Prime minimization of the residues and the ligand for each pose, a Glide SP redocking of each protein−ligand complex structure within 30 kcal/mol above the global minimum was performed. Finally, each output pose was estimated by the binding energy (IFD score) and visually examined. The pretreated 3EQM model was also submitted to a redocking test, evaluating the computational protocol in terms of rmsd deviation onto the ligand coordinates. The rmsd value was equal to 0.18 Å. The 3D Figures 4−6 were obtained with PyMOL graphics and modeling package, version 0.98.[30] The volume analysis of the binding sites has been carried out by means of the FLAPsite utility,[31] as implemented in the FLAP program.[32] The GRID probe was set to DRY, and the other parameters were set as default.

■ ASSOCIATED CONTENT

Ⓢ Supporting Information

Mass spectrometry (MS) analysis for compounds **1**, **2**, **14**, **15**, and **16**; and synthetic procedures as well as spectroscopic and physical data for compounds **6**, **9**, **10**, **12**, **19**, **20**, and **21**. This material is available free of charge via the Internet at http://pubs.acs.org.

■ AUTHOR INFORMATION

Corresponding Author

*Tel: +351 239 488 400. Fax: +351 239 488 503. E-mail: etavares@ff.uc.pt (E.J.T.d.S.); froleira@ff.uc.pt (F.M.F.R.).

Notes

The authors declare no competing financial interest.

■ ACKNOWLEDGMENTS

We thank FCT (Fundação para a Ciência e Tecnologia) for financial support and for the Ph.D. grants for C.V. and C.A. (SFRH/BD/44872/2008 and SFRH/BD/48190/2008, respectively).

■ ABBREVIATIONS USED

AI/AIs, aromatase inhibitors; DRY, GRID hydrophobic probe; 3EQM, PDB code of the aromatase androstenedione crystallographic complex; FLAP, fingerprints for ligands and proteins (molecular software by Molecular Discovery Inc.); Glide, docking software belonging to the Scrodinger suite http://www.schrodinger.com/products/14/5/; GlideSP, Glide single precision version; GRID, software created by Professor Peter Goodford; IFD, induced fit docking; OPLS-AA, optimized potentials for liquid simulations, version all atoms (force field of the Glide software); OPLS-2005, optimized potentials for liquid simulations, version 2005 (force field of the Glide software); PDB, Protein Data Bank; PYMOL, Python-enhanced molecular graphics tool; SEM, standard error of the mean

■ REFERENCES

(1) Winer, E. P.; Hudis, C.; Burstein, H. J.; Wolff, A. C.; Pritchard, K. I.; Ingle, J. N.; et al. American Society of Clinical Oncology Technology Assessment on the Use of Aromatase Inhibitors as Adjuvant Therapy for Postmenopausal Women with Hormone Receptor-Positive Breast Cancer: Status Report 2004. *J. Clin. Oncol.* **2005**, *23*, 619−29.

(2) Perez, E. A. Appraising Adjuvant Aromatase Inhibitor Therapy. *Oncologist* **2006**, *11*, 1058−69.

(3) Jordan, V. C.; Brodie, A. M. H. Development and Evolution of Therapies Targeted to the Estrogen Receptor for the Treatment and Prevention of Breast Cancer. *Steroids* **2007**, *72*, 7−25.

(4) O'Reilly, J. M.; Brueggemeier, R. W. Development of Steroidal and Nonsteroidal Inhibitors of Aromatase for the Treatment of Hormone-Dependent Breast Cancer. *Curr. Med. Chem.* **1996**, *3*, 11−22.

(5) Banting, L.; Nicholls, P. J.; Shaw, M. A.; Smith, H. J. Recent Developments in Aromatase Inhibition as a Potential Treatment for Estrogen-Dependent Breast Cancer. *Prog. Med. Chem.* **1989**, *26*, 253−298.

(6) Banting, L. Inhibition of Aromatase. *Prog. Med. Chem.* **1996**, *33*, 147−184.

(7) Miller, W. R.; Anderson, T. J.; Jack, W. J. L. Relationship between Tumor Aromatase Activity, Tumor Characteristics and Response to Therapy. *J. Steroid Biochem. Mol. Biol.* **1990**, *37*, 1055−1059.

(8) Dutta, U.; Pant, K. Aromatase Inhibitors: Past, Present and Future in Breast Cancer Therapy. *Med. Oncol.* **2008**, *25*, 113−24.

(9) Ghosh, D.; Griswold, J.; Erman, M.; Pangborn, W. Structural Basis for Androgen Specificity and Oestrogen Synthesis in Human Aromatase. *Nature* **2009**, *457*, 219−223.
(10) Cepa, M. D. S.; Tavares-da-Silva, E. J.; Correia-da-Silva, G.; Roleira, F. M. F.; Teixeira, N. A. A. Structure-Activity Relationships of New A,D-Ring Modified Steroids as Aromatase Inhibitors: Design, Synthesis, and Biological Activity Evaluation. *J. Med. Chem.* **2005**, *48*, 6379−6385.
(11) Sherwin, P. F.; McMullan, P. C.; Covey, D. F. Effects of Steroid D-Ring Modification on Suicide Inactivation and Competitive Inhibition of Aromatase by Analogues of Androsta-1,4-diene-3,17-dione. *J. Med. Chem.* **1989**, *32*, 651−658.
(12) Cepa, M. M. D. S.; Tavares da Silva, E. J.; Correia-da-Silva, G.; Roleira, F. M. F.; Teixeira, N. A. A. Synthesis and Biochemical Studies of 17-Substituted Androst-3-enes and 3,4-Epoxyandrostanes as Aromatase Inhibitors. *Steroids* **2008**, *73*, 1409−1415.
(13) Marsh, D. A.; Brodie, H. J.; Garrett, W.; Tsai-Morris, C.; Brodie, A. M. H. Aromatase Inhibitors. Synthesis and Biological Activity of Androstenedione Derivatives. *J. Med. Chem.* **1985**, *28*, 788−795.
(14) Sherman, W.; Day, T.; Jacobson, M. P.; Friesner, R. A.; Farid, R. Novel Procedure for Modeling Ligand/Receptor Induced Fit Effects. *J. Med. Chem.* **2006**, *49*, 534−554.
(15) Zhao, Y.; White, M. A.; Muralidhara, B. K.; Sun, L.; Halpert, J. R.; Stout, C. D. Structure of Microsomal Cytochrome P450 2B4 Complexed with the Antifungal Drug Bifonazole: Insight into P450 Conformational Plasticity and Membrane Interaction. *J. Biol. Chem.* **2006**, *281*, 5973−5981.
(16) Parish, E. J.; Scott, A. D. Selective Oxidation of Steroidal Allylic Alcohols Using 3,5-Dimethylpyrazole and Pyridinium Chlorochromate. *J. Org. Chem.* **1983**, *48*, 4766−4768.
(17) Varela, C. L.; Roleira, F. M. F.; Carvalho, R. A.; Teixeira, N. A. A.; Tavares-da-Silva, E. J. Insights and Mechanisms towards the Reactivity of Steroid A-Ring Δ1- and Δ4−3-Ketoenones and Corresponding Allylic Alcohols, unpublished results.
(18) Oh, S. S.; Robinson, C. H. Synthesis of and Chemical Model Reaction Studies with 3-Deoxyandrogens: Evidence Supporting a 2,3-Enolization Hypothesis in Human Placental Aromatase Catalysis. *J. Chem. Soc., Perkin Trans. 1* **1994**, 2237−2243.
(19) Numazawa, M.; Mutsumi, A.; Hoshi, K.; Koike, R. 19-Hydroxy-4-androsten-17-one: Potential Competitive Inhibitor of Estrogen Biosynthesis. *Biochem. Biophys. Res. Commun.* **1989**, *160*, 1009−1014.
(20) Campbell, M. M.; Craig, R. C.; Boyd, A. C.; Gilbert, I. M.; Logan, R. T.; Redpath, J.; Roy, R. G.; Savage, D. S.; Sleigh, T. Aminosteroids. Part 6. Stereospecific Syntheses of Eight, Isomeric, Steroidal Vicinal 2,3-Amino-alcohols. *J. Chem. Soc., Perkin Trans. 1* **1979**, 2235−2247.
(21) Bowers, A.; Cross, A. D.; Edwards, J. A.; Carpio, H.; Calzada, M. C.; Denot, E. Steroids. CCV. Ring A Modified Hormone Analogs. Part I. Some Ring A Olefins. *J. Med. Chem.* **1963**, *6*, 156−161.
(22) Mohamed, N. R.; Elmegeed, G. A.; Younis, M. Studies on Organophosphorus Compounds VII: Transformation of Steroidal Ketones with Lawesson's Reagent into Thioxo and Heterofused Steroids. Results of Antimicrobial and Antifungal Activity. *Phosphorus, Sulfur Silicon Relat. Elem.* **2003**, *178*, 2003−2017.
(23) Thompson, E. A.; Siiteri, P. K. Utilization of Oxygen and Reduced Nicotinamide Adenine Dinucleotide Phosphate by Human Placental Microsomes during Aromatization of Androstenedione. *Biol. Chem.* **1974**, *249*, 53−64.
(24) Numazawa, M.; Kamiyama, T.; Tachibana, M.; Oshibe, M. Synthesis and Structure-Activity Relationships of 6-Substituted Androst-4-ene Analogs as Aromatase Inhibitors. *J. Med. Chem.* **1996**, *39*, 2245−2252.
(25) Yoshida, N.; Osawa, Y. Purification of Human Placental Aromatase Cytocrome P-450 with Monoclonal Antibody and Its Characterization. *Biochemistry* **1991**, *30*, 3003−3010.
(26) Heidrich, D.; Steckelbroeck, S.; Klingmuller, D. Inhibiton of Human Cytocrome P-450 Aromatase Activity by Butylins. *Steroids* **2001**, *66*, 763−769.
(27) *Maestro*, version 9.1; Schrödinger, LLC: New York, NY, 2010.
(28) Banks, J. L.; Beard, H. S.; Cao, Y.; Cho, A. E.; Damm, W.; Farid, R.; Felts, A. K.; Halgren, T. A.; Mainz, D. T.; Maple, J. R.; Murphy, R.; Philipp, D. M.; Repasky, M. P.; Zhang, L. Y.; Berne, B. J.; Friesner, R. A.; Gallicchio, E.; Levy, R. M. Integrated Modeling Program, Applied Chemical Theory (IMPACT). *J. Comput. Chem.* **2005**, *26*, 1752−1780.
(29) Jorgensen, W. L.; Maxwell, D. S.; Tirado-Rives, J. Development and Testing of the OPLS All-Atom Force Field on Conformational Energetics and Properties of Organic Liquids. *J. Am. Chem. Soc.* **1996**, *118*, 11225−11236.
(30) Delano W. L. The PyMOL Molecular Graphics System, 2002. http://www.pymol.org
(31) Henrich, S.; Salo-Ahen, O. M. H.; Huang, B.; Rippmann, F.; Cruciani, G.; Wade, R. C. Computational Approaches to Identifying and Characterizing Protein Binding Sites for Ligand Design. *J. Mol. Recognit.* **2010**, *23*, 209−219.
(32) Baroni, M.; Cruciani, G.; Sciabola, S.; Perruccio, F.; Mason, J. S. A Common Reference Framework for Analyzing/Comparing Proteins and Ligands. Fingerprints for Ligands and Proteins (FLAP): Theory and Application. *J. Chem. Inf. Model.* **2007**, *47*, 279−294.